From honeycomb- to microsphere-patterned surfaces of poly(lactic acid) and a starch-poly(lactic acid) blend via the breath figure method

Ana Rita C. Duarte[1,2], Devid Maniglio[3], Nuno Sousa[1,2], João F. Mano[1,2], Rui L. Reis[1,2], Claudio Migliaresi[3]

[1] 3Bs Research Group, University of Minho, Caldas das Taipas, Guimarães - Portugal
[2] ICVS/3Bs PT Government Associated Laboratory, Braga/Guimarães - Portugal
[3] Department of Industrial Engineering, BIOtech Research Center, European Institute of Excellence on Tissue Engineering and Regenerative Medicine, University of Trento, Trento - Italy

ABSTRACT

Background: This study investigated the preparation of ordered patterned surfaces and/or microspheres from a natural-based polymer, using the breath figure and reverse breath figure methods.
Methods: Poly(D,L-lactic acid) and starch poly(lactic acid) solutions were precipitated in different conditions – namely, polymer concentration, vapor atmosphere temperature and substrate – to evaluate the effect of these conditions on the morphology of the precipitates obtained.
Results: The possibility of fine-tuning the properties of the final patterns simply by changing the vapor atmosphere was also demonstrated here using a range of compositions of the vapor phase. Porous films or discrete particles are formed when the differences in surface tension determine the ability of polymer solution to surround water droplets or methanol to surround polymer droplets, respectively. In vitro cytotoxicity was assessed applying a simple standard protocol to evaluate the possibility to use these materials in biomedical applications. Moreover, fluorescent microscopy images showed a good interaction of cells with the material, which were able to adhere on the patterned surfaces after 24 hours in culture.
Conclusions: The development of patterned surfaces using the breath figure method was tested in this work for the preparation of both poly(lactic acid) and a blend containing starch and poly(lactic acid). The potential of these films to be used in the biomedical area was confirmed by a preliminary cytotoxicity test and by morphological observation of cell adhesion.

Keywords: Biomaterials, Breath figures, Natural polymers, Patterns, Poly(lactic acid), Starch

Introduction

The first observations on "breath figures" and on the possibility of taking advantage of the spontaneous condensation of water droplets were made by Lord Rayleigh in early 1911 (1). Nonetheless it was only in the last 2 decades that the process has gained more attention from the scientific community (2-5). The possibility of creating highly ordered structures as an alternative to conventional templating technologies has inspired several authors, stimulating their curiosity.

Several conventional templating technologies or microfabrication techniques have been developed for processing different types of materials in a wide variety of shapes for different applications (6, 7). Among these are replication techniques, such as imprinting lithography or soft lithography; rapid prototyping techniques, such as 3-dimensional (3D) printing and laser stereolithography and laser micropatterning (8-10). All of these require very specialized machinery and the production of specific templates and/or molds, which is probably the greatest disadvantage of these processes, due to the inherent high costs. However, once designed, the molds can be applied numerously, and furthermore, they offer a large freedom of design: the master mold can be fabricated with various geometries, which present great advantages in the microfabrication technologies.

To overcome the limitations of these processes, the formation of honeycomb-ordered structures by breath figures may give exciting perspectives (11-14). Breath figure formation takes place with the rapid evaporation of the solvent under a flow of humid air, which leads to the condensation of water droplets on the surface of the substrate and the formation of a self-

Corresponding author:
Devid Maniglio
Department of Industrial Engineering
BIOtech Research Center
Via delle Regole 101
38123 Trento, Italy
devid.maniglio@unitn.it

assembled, ordered, honeycomb film (15). The general mechanism proposed for the formation of a breath figure–patterned surface relies, in this work, on 3 subsequent steps: cooling of the polymer solution by the evaporation of the organic solvent, water condensation from the humid flow and simultaneous arrangement of the water droplets in an ordered hexagonal structure and finally the evaporation of organic solvent and water. Although it is a simple method, a full understanding of the mechanisms that govern the breath figure formation is still the object of discussion (16). The interplay of the thermodynamics and hydrodynamics on the film properties, particularly on the pore size and pore size distribution, has to be investigated further to scale up the process.

The possibility of processing different polymers by the breath figure method has been tested and is described in a number of works reported in the literature. Polymeric blends (17), block copolymers (18, 19), amphiphilic copolymers (20, 21), dendronized polymers (22) and star copolymers (23, 24) are among those reported. Recently, Sun and coworkers reported the use of a stabilizing agent to promote the preparation of highly ordered films (25). The application of such processes for the development of materials to be used in the pharmaceutical and/or biomedical area has not been extensively described. However, the few works reported present promising results. Beattie and coworkers have reported that fibroblast cell attachment in conducting block copolymers is greatly influenced by the presence of an ordered structure prepared by breath figure (18). In another work from the same group, the possibility of preparing surfaces for cell growth was successfully demonstrated (26). Recently, poly(ε-caprolactone) honeycomb structures were reported useful for neural tissue engineering (27). Fukuhira et al reported biodegradable honeycomb-patterned films from poly(lactic acid) and dioleoylphosphatidylethanolamine (DOPE) patterned films, which demonstrated good cell proliferation and were hence proposed as candidate scaffolds for tissue engineering applications (28). Specific applications can greatly benefit from patterned surfaces. Recently, Gerberich and coauthors (29) have reviewed the use of scaffold patterned surfaces for tissue engineering, particularly to be used as antimicrobial surfaces (30), cardiac constructs to establish proper alignment of cardiomyocytes, as neurite outgrowths on 2-dimensional surfaces or to guide stem cell differentiation. The development of patterned surfaces may offer a structuring tool for tissue growth, although the effect of surface features on cell behavior is still a subject of discussion, as many variables influence cell behavior, and some of these variables are difficult to study independently. Ponnusamy et al report the use of breath figure–patterned surfaces as 3D substrates for cell adhesion and growth, particularly to mimic mammary tissue and provide a surface for in vitro cell culturing (31). Breath figures have also been reported to have the potential to regulate cell behavior as described by Wu and coworkers (32) or to induce stem cell differentiation (33). The potential of these systems goes further as deeper knowledge is generated. Wang and coworkers report the antibacterial effect of substrate prepared by the breath figure method (34).

Moreover, under particular circumstances, when casting conditions are opportunely tuned, there is the possibility to switch between highly ordered holed films to a complementary assembly constituted of patterns of polymeric microspheres. Xiong and coworkers have proposed for the first time a method for the preparation of microsphere patterns: the so-called reverse breath figure method (35). The microspheres can be seen as the reverse of the honeycomb structures. Microspheres of linear and star-shaped poly(styrene-block-butadiene) copolymers were produced using this technique. The major difference in the process is the fact that the atmosphere created is composed of an organic solvent rather than water, which traditionally creates the breath figure patterns. In this case, the condensed liquid favors the formation of droplets of the polymeric solution, which solidify in a microsphere pattern. Potential applications of these materials are similar to those of breath figure films but can also include use as micrometric vectors for drug delivery (36).

The use of breath figure methodology to process natural-based polymers has been only recently reported (37). In recent years, biodegradable plastics made from renewable resources constitute an important material innovation because they decrease dependence on petroleum and reduce the amount of waste material. Several naturally derived polymers, such as cellulose, starch, chitosan, chitin, alginates and other polysaccharides, hold the potential to be used in applications where synthetic polymers have been traditionally the materials of choice, as is the case in biomaterials and biomedical applications (38). Processing natural-based polymers still remains a challenging task, due the intrinsic nature of these materials. Their unusually high crystallinity limits their solubility in most organic solvents, and their high melting temperature, which is in most cases higher than the degradation temperature of the polymer, does not allow the use of conventional solvent-based or melt-based processing methodologies. To overcome this, blend natural-polymers with biocompatible thermoplastics such as poly(lactic acid) have been shown to be a promising way to enhance polymer processability. In this work, we hypothesized that the breath figure technique might be employed to prepare honeycomb-ordered films and/or microspheres of natural-based polymers.

Breath figure and reverse breath figure methods can be optimized by tuning particular variables – namely, humidity, solvent, polymer, polymer concentration in solution, temperature, substrate and vapor atmosphere. These parameters were tested in this work. We particularly focused on the possibility of tuning the characteristics of the patterns formed by varying the vapor atmosphere composed of pure water or pure methanol and a range of stoichiometric percentages of both, to give more insights into the mechanisms that govern the breath figure pattern formation.

As a last step, the materials obtained were tested to check their possible use in a biologically oriented application, excluding cytotoxicity issues and evaluating their positive interaction in contact with cells.

Materials and methods

Materials

Poly(D,L-lactic acid) (PDLLA) with an inherent viscosity of 1.87 dL/g was purchased from Boehringer Ingelheim (Resomer R207S, a racemic mixture 50:50) and a commercial blend of

poly(L-lactic acid) and starch (SPLA; 70:30) was obtained from Novamonte. Analytical grade toluene, chloroform (CHCl$_3$) and methanol (MeOH) were purchased from Sigma and Fluka and were used without any further purification.

Reverse breath figure

An in-house built apparatus was used to precipitate PDLLA and SPLA by the reverse breath figure method. Briefly, a constant flow of nitrogen of 5 mL s^{-1} was passed through the bubbler containing the nonsolvent. The bubbler was set to the desired temperature (0°C, room temperature or 50°C), and the nonsolvent composition was a stoichiometric ratio between water and methanol (H$_2$O:MetOH molar ratios tested were 100:0; 80:20; 75:25; 70:30; 50:50; 30:70; 25:75; 20:80 and 0:100). The nitrogen flowed through the chamber in which the substrate was placed, creating a saturated atmosphere and forming small droplets due to condensation. At this point, a droplet of polymeric solution was injected on top of the substrate. The polymers (PDLLA or SPLA) were dissolved in the appropriate solvent (toluene or chloroform) at the desired concentration (0.5 or 1 wt%). The process was repeated changing 1 condition at the time. The different substrates tested were glass, polyethylene terephthalate (PET), Teflon and silicon (with and without patterned surface). All substrates were gently cleaned before casting by immerging in nonionic detergent followed by acetone.

Contact angle measurements

Contact angles of the substrates were measured using a Wilhelmy balance and Milli-Q ultrapure water. The velocity of the movement was adjusted at is 20 µm/s, and each sample was dipped twice (the first immersion for 6 mm, the second for 10 mm) to verify surface wetting stability.

Scanning electron microscope

The samples prepared were characterized by scanning electron microscope (SEM) analysis (NanoSEM - FEI Nova 200 - FEG/SEM). The samples were fixed by mutual conductive adhesive tape on aluminum stubs and covered with gold palladium using a sputter coater.

In vitro studies

Cell culture and seeding

A human osteogenic sarcoma cell line (SaOS-2 cell line; European Collection of Cell Cultures, UK), was maintained in Dulbecco's modified Eagle's medium (DMEM; Sigma-Aldrich, Germany) supplemented with 10% heat-inactivated fetal bovine serum (Biochrom AG, Germany) and 1% antibiotic-antimycotic solution (Gibco, UK). Cells were cultured in a humidified incubator at 37°C in a 5% CO$_2$ atmosphere.

Confluent cells were harvested and seeded in the different surfaces as follows: PDLLA and SPLA matrixes were distributed in a 24-well culture plate. Then 1 mL of cell suspension with a concentration of 4 × 10^4 cells/mL was seeded on top of the surfaces and cultured for 24 and 72 hours. Glass surfaces were used as control.

Cell viability assay

Cell viability was evaluated by the MTS assay. This assay is based on the bioreduction of a tetrazolium compound, 3-(4,5-dimethylthiazol-2-yl)-5-(3-carboxymethoxyphenyl)-2-(4-sulphofenyl)-2H-tetrazolium (MTS; Promega, USA), into a water-soluble brown formazan product. This was quantified by UV spectroscopy, reading the formazan absorbance at 490 nm in a microplate reader (Bio-Tek, Synergie HT, USA). Three samples per time point were analyzed.

Cell adhesion and morphology

Cells were stained with calcein and observed under a fluorescent microscope to evaluate cell distribution and morphology within the surface of the substrate. Green fluorescence is also an indication of the viability of the cells cultured on these matrices.

Results and discussion

The formation of patterned surfaces via the breath figure or reverse breath figure method, although involving a simple experimental method, may be influenced by a vast number of different parameters. In this work we evaluated the effect on the morphology of the structures obtained, of the polymer solution concentration, temperature, substrate effect in different PDLLA solutions and the effect of the solvent and the nonsolvent in the preparation of PDLLA and SPLA patterned surfaces.

Figure 1 shows the SEM micrographs of the particles prepared at 50°C, from PDLLA solutions in toluene and chloroform (0.5 and 1 wt%) and different substrates (glass, PET, Teflon, silicon and patterned silicon). The main parameters tested were, hereafter, polymer concentration, temperature of the vapor atmosphere and substrate. Methanol was used to create the vapor atmosphere and therefore to act as nonsolvent. Methanol was chosen, instead of ethanol, due to its higher surface tension, as well as other advantages, which give it the potential to lead to better results.

Effect of polymer concentration

The polymer concentration in solution is an important parameter that needs to be optimized to produce discrete microspheres, as the process depends on the mobility of the condensed droplets from the vapor phase. Two polymer solutions were tested, at 2 different concentrations. PDLLA was dissolved in toluene and chloroform at 0.5 and 1 wt%. Experiments suggest that a concentration of 0.5 wt% is too low for the preparation of microspheres. For this reason, 1 wt% of polymer concentration in solution was used in the following experiments.

Effect of temperature of vapor atmosphere

The breath figure formation mechanism relies on the creation of patterns by the condensation phenomenon. These
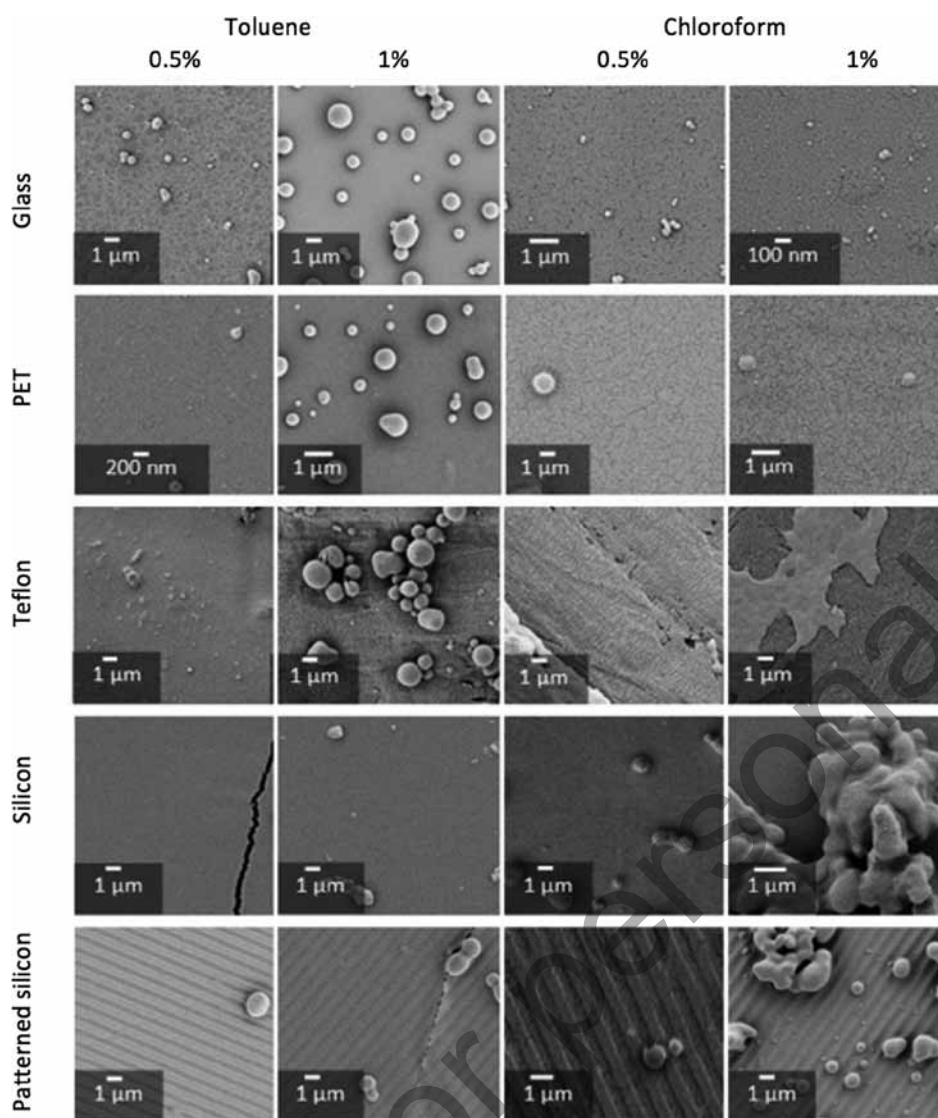
Fig. 1 - Poly(lactic acid) (PDLLA) particles formed using different experimental conditions – namely, polymer solution, polymer concentration and substrate (all experiments were carried out in a methanol vapor atmosphere at 50°C). PET = polyethylene terephthalate.

patterns are formed when moist air comes in contact with a cold surface. The temperature of the vapor phase atmosphere will influence the facility to form the patterns described (35). In physical terms, an increase in temperature corresponds to a decrease in surface tension, which is translated into a higher mobility. Experiments were carried out at 0°C, room temperature and 50°C for the precipitation of PDLLA from toluene or chloroform solution. At lower temperatures, the preparation of particles was not successful due to the poor saturation of vapor atmosphere with the methanol and consequently the condensation of methanol on the substrate surface (see supplementary material). The increase to 50°C seemed to promote the best conditions for the successful formation of particles; therefore, this condition was used in subsequent experiments.

Effect of substrate

In this work, substrates from glass, PET, Teflon, silicon and a patterned surface of silicon were tested. The results obtained

and presented in Figure 1 suggest that microspheres formation was favored when glass and PET substrates were used. Different substrates produce different morphological characteristics. However, the relationship between this parameter and the type of structures prepared is still an object of discussion, and a consensus has not yet been reached among the scientific community. It may be explained by the differences in wettability of the surfaces, which seems to be the characteristic that governs the differences obtained (39). We evaluated, hereafter, the contact angles of the surfaces to investigate the surface energy of the substrates. Contact angles measured in the substrates tested showed that in terms of magnitude, the contact angles showed the following inequalities: silicon <glass <PET <Teflon – namely, 52 ± 1, 69 ± 4, 94 ± 5, 121 ± 7, respectively. These observations suggest that in the particular case of precipitation of PDLLA from organic solutions, the best substrates for reverse breath figure formation are the ones with lower contact angles (silicon and glass) – that is, substrates presenting higher wettability. The substrate chosen to pursue the objectives of this work and to perform subsequent experiments was glass.
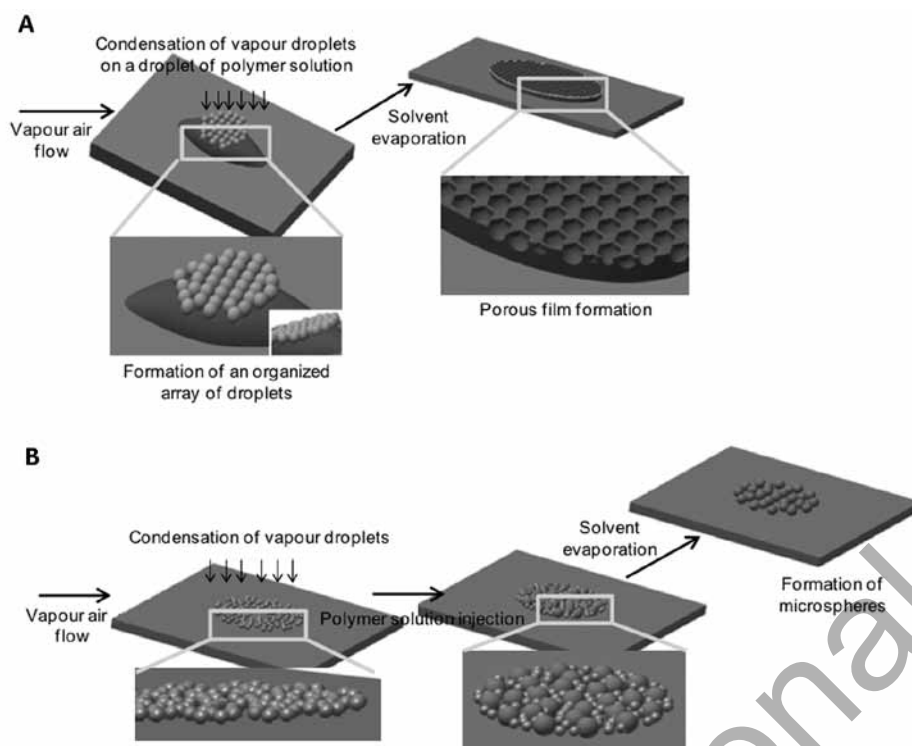
Fig. 2 - Schematics of the different stages of the process of breath figure (**A**) and reverse breath figure (**B**) formation.

TABLE I - Physical properties of solvents and nonsolvents used in study

	Density 20°C (g/cm³)	Viscosity 25°C (mPa/s)	Solubility in water 20°C (g/100 mL)	Interfacial tension with water 25°C (mN/m)	Boiling point (°C)	Vapor pressure 25°C (kPa)	Enthalpy of vaporization (kJ/mol)
Toluene	0.87	0.56	0.05	36.1	111	3.8	38.0
Chloroform	1.48	0.54	0.8	33.5	61	26.2	31.3
Water	0.99	0.89	-	-	100	3.2	43.9
Methanol	0.79	0.54	27	-	65	16.4	35.3

Data from reference (40).

Having determined the best conditions which concern polymer concentration (1 wt%), temperature of vapor phase (50°C) and substrate (glass), we investigated the effects of solvent and composition of the vapor atmosphere.

Solvent and vapor atmosphere effect

The formation of a honeycomb-ordered morphology structure pattern by the breath figure method has been described to occur in 3 stages. In the initial stage, nucleation and growth of the nonsolvent droplets occurs. This step is mainly governed by the type of nonsolvent used and the temperature of the environment. The second stage involves surface arrangement of nonsolvent droplets into a hexagonal array, and the third regards polymer precipitation around the nonsolvent, followed by complete evaporation of the solvent. Contrary to the first 2 steps, this last one is greatly influenced

by the nature of the polymer itself. The same steps occur in the reverse breath figure method, although in the second stage, it is the polymeric solution that forms the droplets involved by the nonsolvent (26). Figure 2 schematically represents these stages of breath figure formation and reverse breath figure formation. The differences in the processes are related to the interface phenomena that occur between polymer/solvent/nonsolvent. The physical properties of the solvents and nonsolvents and the affinity toward the polymer greatly affect the breath figure and reverse breath figure process. Table I presents the physical properties of the solvents and nonsolvents used in this study.

Depending on the surface properties such as surface tension of solution and nonsolvent, the process will occur when 1 or the other liquid wets better the substrate surface; hereafter, the liquid with lowest surface tension will be considered the continuous phase, surrounding the liquid
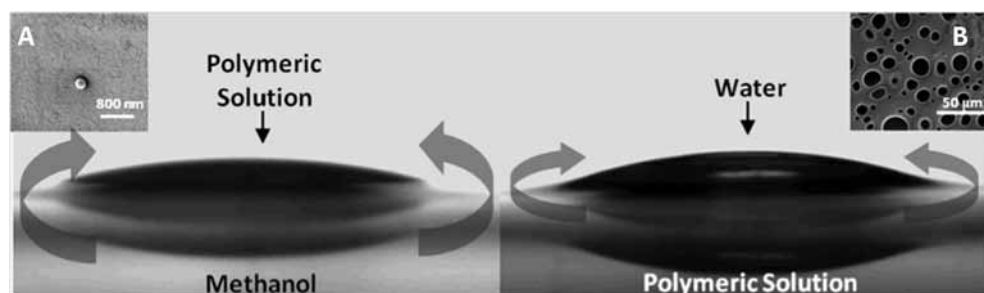
Fig. 3 - (**A**) Poly(lactic acid) (PDLLA)-toluene drop over 50:50 of MeOH:Water solution for contact angle measurement, resulting in a "sphere"; (**B**) 25:75 MeOH:Water solution drop over PDLLA-toluene for contact angle measurement, resulting in porous film.
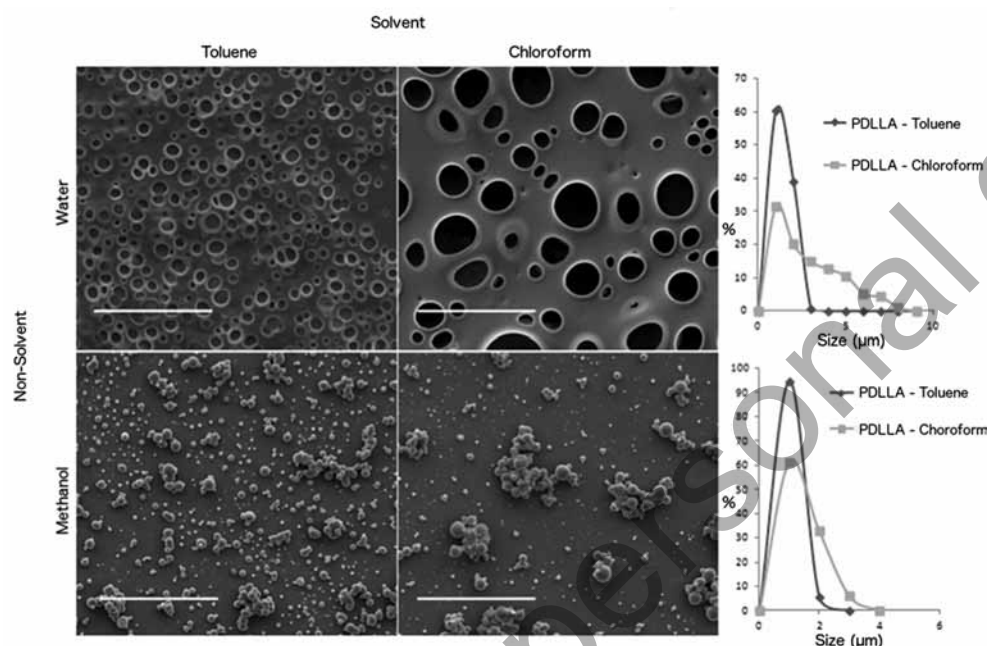

Fig. 4 - Poly(lactic acid) (PDLLA) structures created and their size distribution (scale bar: 20 µm).

with higher surface area. Figure 3 shows the differences in the processes.

In the case of microsphere formation, the condensed liquid (methanol) spreads, and the polymer solution shrinks to form microdroplets due to its higher surface tension (Fig. 3A). In contrast, in the case of polymeric film formation, the surface tension of the vapor phase (water) is higher than that of the polymeric solution, the condensed liquid forms stable drops at the surface and porous films are obtained (Fig. 3B).

The choice of the best organic solvent to precipitate polymers using the breath figure and reverse breath figure methods strongly depends on the capability of the solvent to dissolve the polymer and on the affinity of the polymer toward the solvent. Its effect on the reverse breath figure formation is, however, more complex; it is related to the physical properties of the solvents and the thermodynamic affinity toward polymer and composition of vapor atmosphere. Two different solvents, toluene and chloroform, and 2 nonsolvents (water and methanol) were used, and the effect on the precipitation of PDLLA and SPLA was evaluated (Figs. 4 and 5, respectively). For both polymers and polymeric solutions, ordered porous films were obtained when water was used in a condensed phase, while microspheres

were collected after the precipitation using methanol to create the vapor atmosphere.

Image analysis allowed the determination of the pore and particle size distribution from the SEM images. In the case of the films, the precipitation from toluene solution generated a more homogeneous pattern with a narrow pore size distribution (Figs. 4 and 5). This was observed for both polymers. Honeycomb-patterned surfaces were only achieved for the natural-based polymer, and the most ordered structure was obtained from SPLA precipitated from toluene solution. The formation of honeycomb structures has been considered to depend on – besides interfacial phenomena – the thermodynamic affinity between polymer and solvent and solvent-nonsolvent (41). In this work, we studied the affinity between polymer and solvent based of the Hansen solubility parameters (HSPs) (42). The solubility parameter is one of the most widely applicable scales, reflecting the total Van der Waals forces between molecules. The solubility parameter is also an important parameter, as it is a function of the cohesive energy density. The approach followed is based on the degree of compatibility of materials – i.e., on the relative energy difference (RED), which can be estimated from the different interaction parameters between polymer and solvent using Equation [1]:
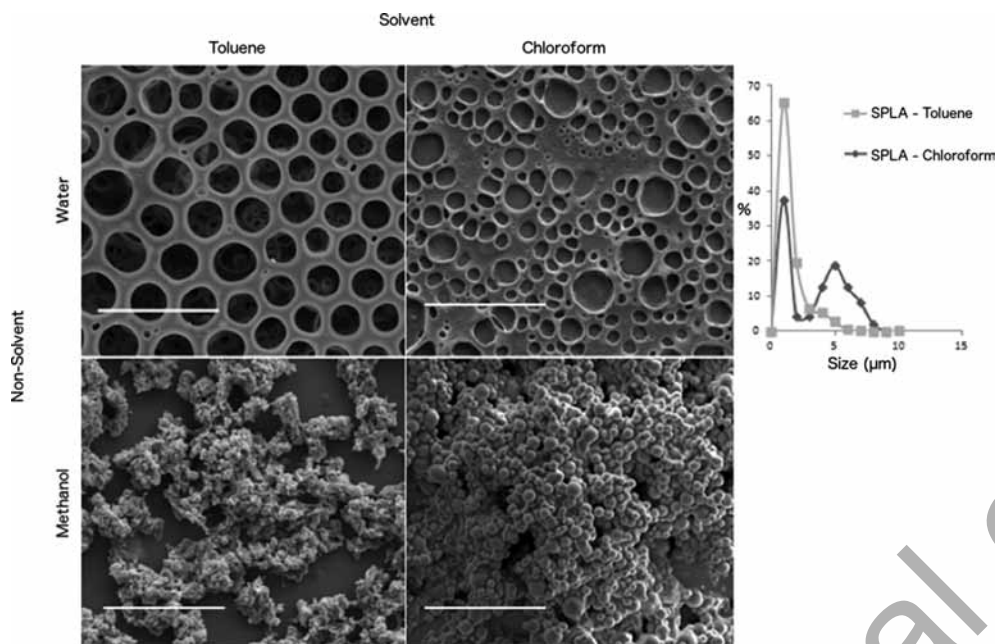
Fig. 5 - Blend containing starch and poly(lactic acid) (SPLA) structures created and their size distribution (scale bar: 20 µm).

$$RED = \frac{\left[4(\delta D_s - \delta D_p)^2 + (\delta P_s - \delta P_p)^2 + (\delta H_s - \delta H_p)^2\right]^{1/2}}{Radius}$$ Eq. [1]

where, δ_D, δ_P and δ_H are the HSPs, as listed in Table II.

The lack of information on the physical constants for the polymeric blend of starch-poly(lactic acid) limits the analysis to the pure synthetic polymer PDLLA; however, this can still provide us with some insights into the thermodynamic parameters influencing the breath figure and reverse breath figure methods. The estimated values for RED between PDLLA-toluene and PDLLA-chloroform were <1 (Tab. II). These values provide an indication that there is a high thermodynamic affinity between polymer and solvent, and therefore the ability to form ordered breath figures (41, 44). Additionally, toluene is the solvent with a lower vapor pressure, higher surface tension and higher RED, which suggests that toluene is a good solvent for the preparation of highly ordered structures from PDLLA. The patterned surfaces obtained from the breath figure process are dependent on the compatibility between polymers and solvents, thus, a poor solvent is the one that allows the migration of polymer chains to the water/solution interface, resulting in coalescence of water droplets and poor regularity of pores. The Flory-Huggins interaction parameter, which is commonly used to measure the polymer/solvent compatibility, can also be used to evaluate the compatibility between solvent/nonsolvent and polymer/nonsolvent. The interactions and affinities between solvent and nonsolvent can be calculated using Equation [2]:

$$X = \frac{V_m}{RT}(\delta D_s - \delta D_p)^2 + (\delta P_s - \delta P_p)^2 + (\delta H_s - \delta H_p)^2\right]$$ Eq. [2]

where R is the ideal gas constant (8.314 J K^{-1} mol^{-1}), T is the environmental temperature (298 K) and V_m is the molar volume

TABLE II - Affinity parameters for PDLLA, solvents and nonsolvents

	δD	δP	δH	Radius	RED	χ
PDLLA	18.6	9.9	6	10.7	-	-
Toluene	18	1.4	2	-	0.89	3.81
Chloroform	17.8	3.1	5.7	-	0.642	1.53
Water	15.6	16	42.3	-	-	9.91
Methanol	14.7	12.3	22.3	-	-	4.69

From sources (40, 42, 43).
PDLLA = poly(lactic acid); RED = relative energy difference.

TABLE III - Affinity coefficient values (χ) for nonsolvent/solvent

	Toluene	Chloroform
Water	13.40	10.98
Methanol	8.85	6.04

of the solvent or nonsolvent (45, 46). Table III presents the calculated X affinity coefficients for the solvent and nonsolvents used.

The precipitation step is a critical step for the preparation of ordered films. If precipitation is slow, water droplets may coalesce leading to broader pore size distributions. In this sense, it is possible to infer the velocity of solution evaporation from the affinity between solvent and nonsolvent. If the affinity between them is too high, water droplets condense on the surface, but they do not have time to arrange themselves into a regular pattern, resulting in a poorly organized structure. The solvent with faster evaporation will lead to misarranged results. Chloroform, due to its higher vapor pressure and lower boiling point as compared with toluene,
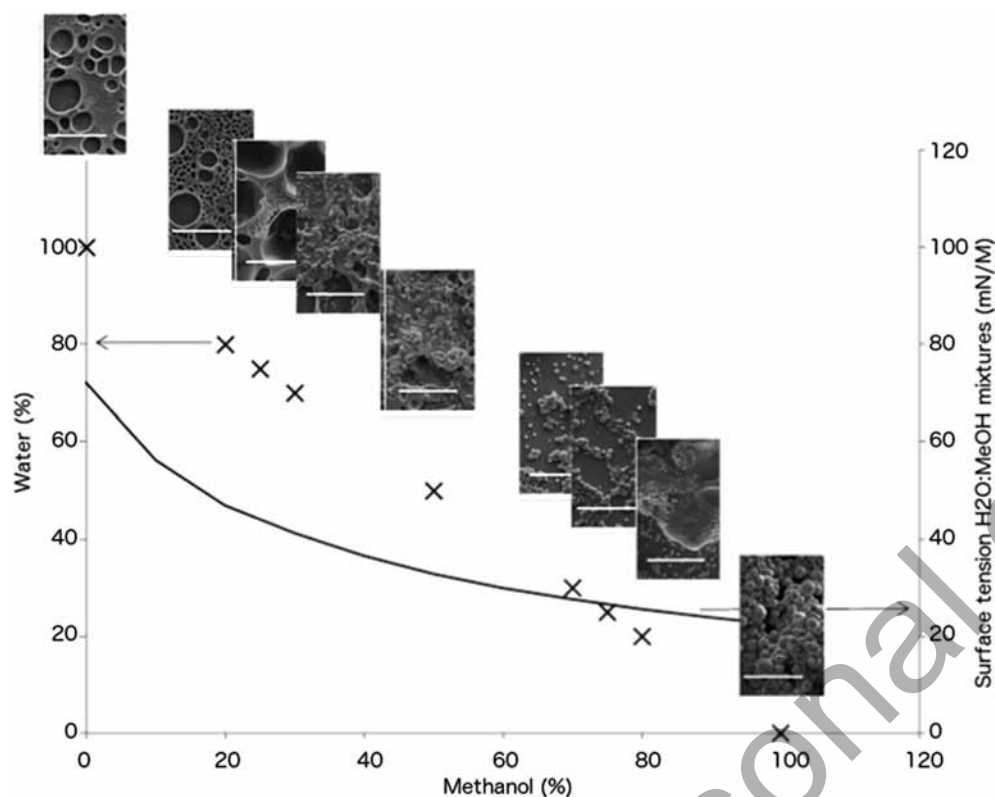
Fig. 6 - Scanning electron microscope images of the different patterns formed with blend containing starch and poly(lactic acid) (SPLA) (from chloroform solution) when using different stoichiometric percentages of water to methanol in the vapor phase (scale bar 10 μm).

will consequently lead to a faster process and therefore to the precipitation of structures with broader pore sizes.

This was also observed for the SPLA breath figure formation. When methanol was used as a nonsolvent, microspheres were created. The differences obtained when using toluene or chloroform can be explained using the same rational as for the SPLA polymeric films. In the reverse breath figure method, the polymer solution will form dispersed small amounts surrounded by a thin layer of nonsolvent. In this case, a faster process leads to the formation of particle agglomerates rather than discrete particles.

After studying the effect of pure vapor atmospheres, the effect of a mixed vapor atmosphere of different methanol to water ratios in the precipitation of PDLLA and SPLA was evaluated. Using the same experimental set up, PDLLA and SPLA dissolved in toluene and chloroform (1 wt%) were cast on a glass substrate under a vapor atmosphere (at 50°C) with different molar percentages of methanol and water. Figure 6 shows the structures obtained for the different conditions tested, regarding SPLA precipitation from toluene solution.

The trend of the morphologies obtained was similar for all conditions studied: both PDLLA and SPLA precipitated in these structures from either toluene or chloroform solutions. The increase in methanol concentration led to the production of spheres, while the presence of a higher percentage of water in the vapor phase led to the development of more or less ordered porous films, as discussed previously.

The coexistence of both nonsolvents leads to the creation of intermediate patterns, in which both a porous film and microspheres are observed. Leong and coworkers (47)

recently described the production of porous films and microspheres of block glyco-copolymers by the addition of water to the polymeric solution. The vapor atmosphere was in this case composed of 28% or 76% humidity. According to their findings, the production of microspheres was only achieved when higher contents of water were added to the polymeric solution. Our results showed the opposite effect. The increase of water content in the vapor atmosphere had a positive effect on the preparation of ordered porous films, while its absence promoted the precipitation of the polymers in a microsphere pattern. This may be explained by the difference in solvents used as well as by the differences in the polymers. In another work, on the preparation of breath figures from a nonaqueous vapor atmosphere, Ding and coworkers (48) have demonstrated the possibility of preparing breath figures either in the presence of organic alcohols such as methanol and ethanol or in the presence of water. The differences obtained in the morphology of the surfaces are related to the size and shape of the pores, which are a function of the physical properties of the atmosphere solvents, including surface tension and evaporation enthalpy.

In vitro studies

The effects of ordered structures on cell attachment and growth has been analyzed by different authors (49). Regular topographies or surface roughness are known to have an influence on cell alignment, can dictate cell migration and can even regulate cell signaling. Ponnusamy and coworkers report the preparation of PLGA porous membranes by the breath
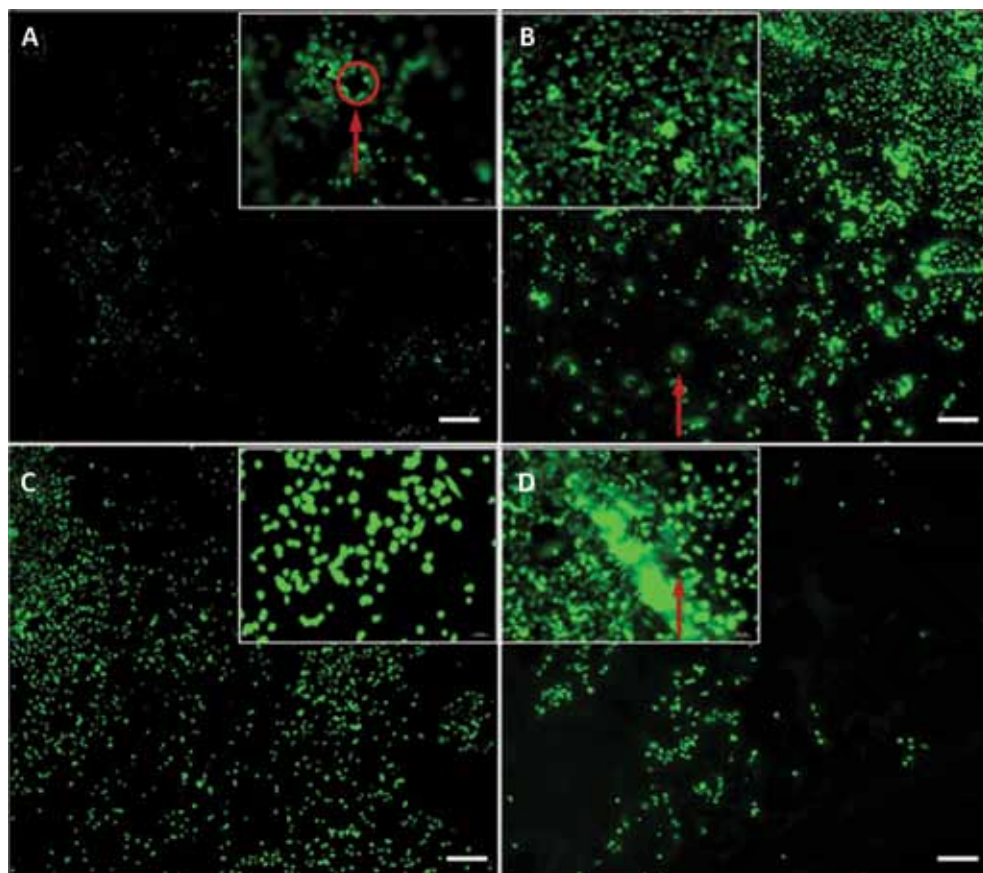
Fig. 7 - Cell growth on poly(lactic acid) (PDLLA) structures: porous film after 24 hours (**A**) and after 72 hours (**B**); and spheres after 24 hours (**C**) and after 72 hours (**D**) (scale bar 200 µm).

figure method for cell growth, particularly for in vitro modeling of mammary morphogenesis. The authors report changes in cell growth and proliferation depending on the topological features of the substrate. The increased porosity provides a large surface area responsible for aggregation of the cells in a 3D orientation, which holds the potential to be used for in vitro substrates which mimic in vivo tissues (31).

In this present study, preliminary experiments on cell attachment, morphology and viability on both PDLLA and SPLA surfaces were assessed by fluorescent microscopy after 24 and 72 hours of culture. Figure 7 shows calcein acetoxymethyl (calcein AM) staining of the cells cultured on PDLLA patterned surfaces after 24 and 72 hours, in both honeycomb-like films and microparticles.

Although the pattern is not clear in these microscopic images, it is possible to notice the arrangement of the cells close to the material, which differs from the shape they have when attached to the glass substrate. While after 24 hours, osteoblasts present a spherical shape when cultured on the material, they are already elongated when growing on the glass surface.

Nevertheless, the good integration of the cells with the materials prepared is also visible by SEM. Figure 8 presents an image of osteoblast cells cultured on SPLA precipitated from toluene solution using 100% methanol in the vapor phase. That image shows that after 72 hours, the cells are spread on the surfaces developed. The cells are well spread, and the particles have promoted cell attachment. Furthermore, it
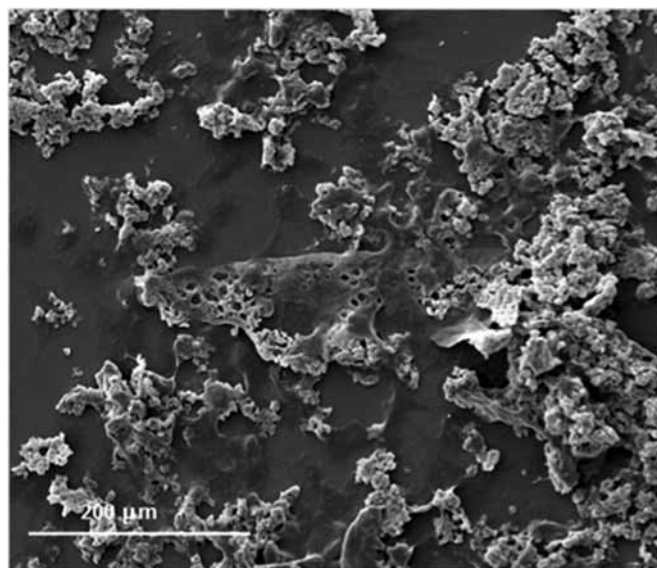

Fig. 8 - Scanning electron microscope image of cell growth on microspheres from blend containing starch and poly(lactic acid) (SPLA), after 72 hours of culture.

is possible to observe that they follow the contour of the pattern.

The preparation of substrates for cell culture and growth with potential applications in tissue engineering involves
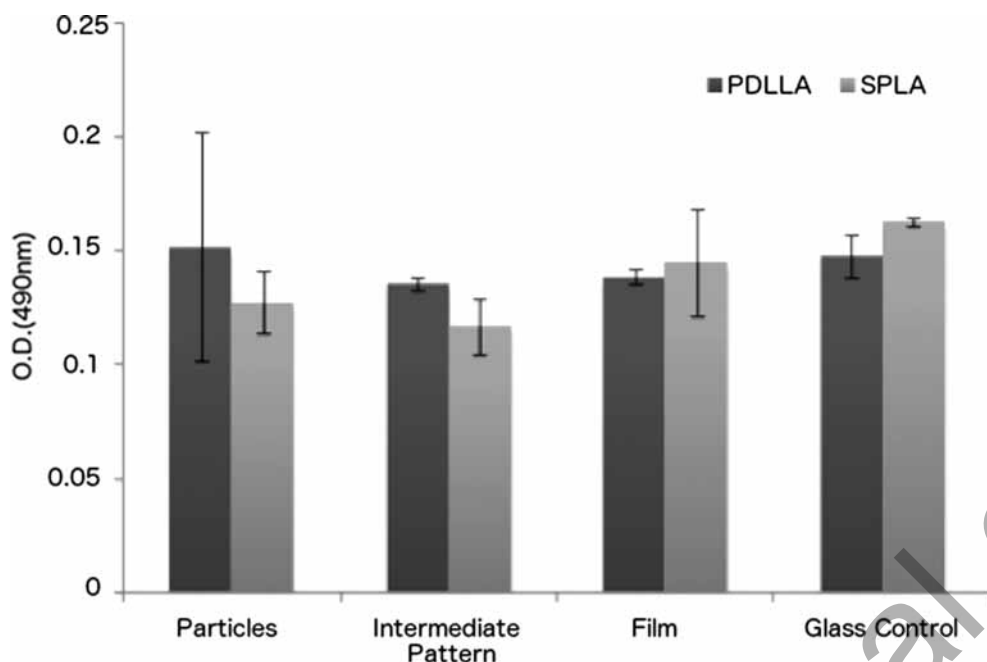
Fig. 9 - Cytotoxicity screening of the poly(lactic acid) (PDLLA) matrices produced from a chloroform solution and blend containing starch and poly(lactic acid) (SPLA) from a toluene solution, after 24 hours of in vitro cell culture.

rigorous control of the potential toxic compounds that may be present, and this is particularly relevant when organic solvents are used in the preparation of the materials. In vitro cytotoxicity studies were carried out on 3 different substrates produced. Cytotoxicity of samples of PDLLA prepared from a chloroform solution and SPLA prepared from a toluene solution were evaluated by MTS assay, after 24 hours of cell culture. Figure 9 shows the viability of cells when compared with the control (glass surface).

The results demonstrate that the cells are able to attach to the materials produced, and no significant differences between cell growth on the surfaces and on the polystyrene culture plate were observed. Therefore we can conclude that the materials produced do not induce a cytotoxic effect on cell growth.

Conclusions

The development of patterned surfaces using the breath figure method was tested in this work for the preparation of both PDLLA and a blend containing starch and poly-lactic acid (SPLA). The best conditions to process PDLLA and SPLA patterns and the influence of different parameters, such as temperature or concentration of the solutions, and the different substrates, were evaluated. The results suggest that higher temperatures of the vapor phase favor the process (50°C). The wettability properties of glass also show that this is the best substrate for the experiments performed. The solvent used in the preparation of polymer solution also had an effect on the patterned surfaces prepared, with toluene being the better solvent, especially due to its lower thermodynamic affinity toward the polymer and higher affinity toward the solvent used in the vapor phase, when compared with chloroform.

We have demonstrated that the preparation of a honeycomb-ordered film or a microsphere pattern from PDLLA and SPLA depends largely on the vapor phase atmosphere. Ranging from pure water to pure methanol in the vapor phase, highly ordered porous membranes or microspheres were obtained. According to the results obtained, the process is governed by interplay of different conditions such as the polymeric solution and vapor phase characteristics. In particular, interfacial tension between the evaporating solvent and the condensing nonsolvent present in the vapor atmosphere mainly account for the type and organization of the structures created. The ability of polymer solution to surround water droplets, or methanol to surround polymer droplets, will ultimately determine whether a porous film or particles are formed.

The potential of these films to be used in the biomedical area was confirmed by a preliminary cytotoxicity test and by morphological observation of cell adhesion. These structures may be used in different applications. In particular, they present an interesting alternative to bottom-up approaches, which involve microfabrication techniques for the development of 3D structures by assembly of different polymeric layers. The experimental designs used and the general principles that resulted from the analysis of the results could be used in the development of patterned surfaces with other systems.

Acknowledgement

Disclosures

Conflict of interest: None of the authors has any financial interest related to this study to disclose.

References

1. Rayleigh. Breath figures. Nature. 1911;86(2169):416-418.
2. Ma H, Hao J. Ordered patterns and structures via interfacial self-assembly: superlattices, honeycomb structures and coffee rings. Chem Soc Rev. 2011;40(11):5457-5471.
3. Xiong X, Lin M, Zou W. Honeycomb structured porous films prepared by the method of breath figure: history and development. Curr Org Chem. 2011;15(21):3706-3718.
4. Hernandez-Guerrero M, Stenzel MH. Honeycomb structured polymer films via breath figures. Polym Chem. 2012;3(3): 563-577.
5. Munoz-Bonilla A, Fernandez-Garcia M, Rodriguez-Hernandez J. Towards hierarchically ordered functional porous polymeric surfaces prepared by the breath figures approach. Prog Polym Sci. 2014;39(3):510-554.
6. Khademhosseini A, Bettinger C, Karp JM, et al. Interplay of biomaterials and micro-scale technologies for advancing biomedical applications. J Biomater Sci Polym Ed. 2006;17(11):1221-1240.
7. Khademhosseini A, Langer R, Borenstein J, Vacanti JP. Microscale technologies for tissue engineering and biology. Proc Natl Acad Sci USA. 2006;103(8):2480-2487.
8. Borenstein JT, Weinberg EJ, Orrick BK, Sundback C, Kaazempur-Mofrad MR, Vacanti JP. Microfabrication of three-dimensional engineered scaffolds. Tissue Eng. 2007;13(8):1837-1844.
9. Lu Y, Chen SC. Micro and nano-fabrication of biodegradable polymers for drug delivery. Adv Drug Deliv Rev. 2004;56(11): 1621-1633.
10. Park H, Cannizzaro C, Vunjak-Novakovic G, Langer R, Vacanti CA, Farokhzad OC. Nanofabrication and microfabrication of functional materials for tissue engineering. Tissue Eng. 2007;13(8):1867-1877.
11. Bunz UH. Breath figures as a dynamic templating method for polymers and nanomaterials. Adv Mater. 2006;18(8): 973-989.
12. Nurmawati MH, Ajikumar PK, Renu R, Valiyaveettil S. Hierarchical self-organization of nanomaterials into two-dimensional arrays using functional polymer scaffold. Adv Funct Mater. 2008;18(20):3213-3218.
13. Zhang Y, Wang C. Micropatterning of proteins on 3D porous polymer films fabricated by using the breath-figure method. Adv Mater. 2007;19(7):913-916.
14. Escale P, Rubatat L, Billon L, Save M. Recent advances in honeycomb-structured porous polymer films prepared via breath figures. Eur Polym J. 2012;48(6):1001-1025.
15. Srinivasarao M, Collings D, Philips A, Patel S. Three-dimensionally ordered array of air bubbles in a polymer film. Science. 2001;292(5514):79-83.
16. Servoli E, Ruffo GA, Migliaresi C. Interplay of kinetics and interfacial interactions in breath figure templating: a phenomenological interpretation. Polymer (Guildf). 2010;51(11): 2337-2344.
17. Madej W, Budkowski A, Raczkowska J, Rysz J. Breath figures in polymer and polymer blend films spin-coated in dry and humid ambience. Langmuir. 2008;24(7):3517-3524.
18. Beattie D, Wong KH, Williams C, et al. Honeycomb-structured porous films from polypyrrole-containing block copolymers prepared via RAFT polymerization as a scaffold for cell growth. Biomacromolecules. 2006;7(4):1072-1082.
19. Lin CL, Tung PH, Chang FC. Synthesis of rod-coil diblock copolymers by ATRP and their honeycomb morphologies formed by the 'breath figures' method. Polymer (Guildf). 2005;46(22): 9304-9313.
20. Zhu Y, Sheng R, Luo T, et al. Honeycomb-structured films by multifunctional amphiphilic biodegradable copolymers: surface morphology control and biomedical application as scaffolds for cell growth. ACS Appl Mater Interfaces. 2011;3(7): 2487-2495.
21. Wu BH, Zhu LW, Ou Y, Tang W, Wan LS, Xu ZK. Systematic investigation on the formation of honeycomb-patterned porous films from amphiphilic block copolymers. J Phys Chem C. 2015;119(4):1971-1979.
22. Connal LA, Vestberg R, Hawker CJ, Qiao GG. Dramatic morphology control in the fabrication of porous polymer films. Adv Funct Mater. 2008;18(22):3706-3714.
23. Dong W, Zhou Y, Yan D, Mai Y, He L, Jin C. Honeycomb-structured microporous films made from hyperbranched polymers by the breath figure method. Langmuir. 2009;25(1):173-178.
24. Karikari AS, Williams SR, Heisey CL, Rawlett AM, Long TE. Porous thin films based on photo-cross-linked star-shaped poly(D,L-lactide)s. Langmuir. 2006;22(23):9687-9693.
25. Sun W, Shao Z, Ji J. Particle-assisted fabrication of honeycomb-structured hybrid films via breath figures method. Polymer (Guildf). 2010;51(18):4169-4175.
26. Stenzel MH, Barner-Kowollik C, Davis TP. Formation of honeycomb-structured, porous films via breath figures with different polymer architectures. Journal of Polymer Science Part A Polymer Chemistry. 2006;44:2363-2375.
27. Tsuruma A, Tanaka M, Fukushima N, Shimomura M. Morphological changes in neurons by self-organized patterned films. e-Journal of Surface Science and Nanotechnology. 2005;3:159-164.
28. Fukuhira Y, Kitazono E, Hayashi T, et al. Biodegradable honeycomb-patterned film composed of poly(lactic acid) and dioleoylphosphatidylethanolamine. Biomaterials. 2006;27(9):1797-1802.
29. Gerberich BG, Bhatia SK. Tissue scaffold surface patterning for clinical applications. Biotechnol J. 2013;8(1):73-84.
30. Jiang X, Zhang T, He S, et al. Bacterial adhesion on honeycomb-structured poly(L-lactic acid) surface with ag nanoparticles. J Biomed Nanotechnol. 2012;8(5):791-799.
31. Ponnusamy T, Chakravarty G, Mondal D, John VT. Novel "breath figure"-based synthetic PLGA matrices for in vitro modeling of mammary morphogenesis and assessing chemotherapeutic response. Adv Healthc Mater. 2014;3(5):703-13.
32. Wu XH, Wang SF. Integration of photo-crosslinking and breath figures to fabricate biodegradable polymer substrates with tunable pores that regulate cellular behavior. Polymer (Guildf). 2014;55(7):1756-1762.
33. Kawano T, Sato M, Yabu H, Shimomura M. Honeycomb-shaped surface topography induces differentiation of human mesenchymal stem cells (hMSCs): uniform porous polymer scaffolds prepared by the breath figure technique. Biomater Sci-Uk. 2014;2(1):52-56.
34. Wang Y, Liu Y, Li G, Hao J. Porphyrin-based honeycomb films and their antibacterial activity. Langmuir. 2014;30(22):6419-6426.
35. Xiong X, Zou W, Yu Z, et al. Microsphere pattern prepared by a "reverse" breath figure method. Macromolecules. 2009; 42(23):9351-9356.
36. Freiberg S, Zhu XX. Polymer microspheres for controlled drug release. Int J Pharm. 2004;282(1-2):1-18.
37. Galeotti F, Andicsova A, Yunus S, Botta C. Precise surface patterning of silk fibroin films by breath figures. Soft Matter. 2012;8(17):4815-4821.

38. Mano JF, Silva GA, Azevedo HS, et al. Natural origin biodegradable systems in tissue engineering and regenerative medicine: present status and some moving trends. J R Soc Interface. 2007; 4(17):999-1030.

39. Cheng CX, Tian Y, Shi YQ, Tang RP, Xi F. Porous polymer films and honeycomb structures based on amphiphilic dendronized block copolymers. Langmuir. 2005;21(14):6576-6581.

40. Lide DR. CRC handbook of chemistry and physics. 80th ed. Boca Raton, FL: CRC Press; 1999.

41. Tian Y, Jiao QZ, Ding HY, Shi YQ, Liu BQ. The formation of honeycomb structure in polyphenylene oxide films. Polymer (Guildf). 2006;47(11):3866-3873.

42. Hansen CM. Hansen solubility parameters: a user's handbook. Boca Raton, FL: CRC Press; 1999.

43. Siemann U. The solubility parameter of poly(DL-lactic acid). Eur Polym J. 1992;28(3):293-297.

44. Ferrari E, Fabbri P, Pilati F. Solvent and substrate contributions to the formation of breath figure patterns in polystyrene films. Langmuir. 2011;27(5):1874-1881.

45. Flory PI. Thermodynamics of high polymer solutions. J Chem Phys. 1942;10(1):51-61.

46. Flory PJ, Krigbaum WR. Thermodynamics of high polymer solutions. Annu Rev Phys Chem. 1951;2(1):383-402.

47. Leong MF, Chian KS, Mhaisalkar PS, Ong WF, Ratner BD. Effect of electrospun poly(D,L-lactide) fibrous scaffold with nanoporous surface on attachment of porcine esophageal epithelial cells and protein adsorption. J Biomed Mater Res A. 2009;89(4): 1040-1048.

48. Ding J, Zhang A, Bai H, Li L, Li J, Ma Z. Breath figure in non-aqueous vapor. Soft Matter. 2013;9(2):506-514.

49. Alves NM, Pashkuleva I, Reis RL, Mano JF. Controlling cell behavior through the design of polymer surfaces. Small. 2010;6(20): 2208-2220.